Journal of Alloys and Compounds 509 (2011) 3967–3971

Contents lists available at ScienceDirect

Journal of Alloys and Compounds

journal homepage: www.elsevier.com/locate/jallcom

Investigation of structure and magnetization reversal in mechanically alloyed $SmCo_{6.8}Zr_{0.2}$ magnets

Z. Liu*, R.J. Chen, D. Lee, A.R. Yan

Zhejiang Provincial Key Laboratory of Magnetic Materials and Application Technology, Key Laboratory of Magnetic Materials and Devices, Ningbo Institute of Material Technology & Engineering, Chinese Academy of Science, Ningbo 315201, Zhejiang, People's Republic of China

ARTICLE INFO

Article history:
Received 21 April 2010
Received in revised form
27 December 2010
Accepted 29 December 2010
Available online 4 January 2011

Keywords:
SmCo
Nanocrystalline magnetic materials
Inter-grain exchange coupling
Magnetization reversal
Irreversible nucleation field

ABSTRACT

Nanocrystalline $SmCo_{6.8}Zr_{0.2}$ permanent magnets are prepared by intensive milling and subsequent annealing. XRD patterns of the samples annealed at 600 °C and 700 °C show a single $SmCo_7$ phase with $TbCu_7$ structure, while the $SmCo_7$ phase decomposes into a mixture of Sm_2Co_{17} and $Co_{23}Zr_6$ phase at higher annealing temperatures. The highest coercivity and energy product of about 2.06 T and 9.5MGOe are obtained in the sample annealed at 700 °C for 10 min. Further analysis reveals that a very strong inter-grain exchange coupling is observed in samples annealed at 700 °C for 3 (SZ-3) and 10 (SZ-10) min, indicating by the high remanence ratio and positive δm in henkel-plot. It was supposed that the magnetization reversal process is controlled by domain wall pinning.

1. Introduction

Commercial Sm–Co–Fe–Cu–Zr 2:17 magnets have attracted considerable interest for high-temperature applications because of their large energy products and high-temperature performances [1]. Recently, nanocrystalline $SmCo_7$ type permanent magnetic materials have attracted much attention for its excellent permanent magnetic properties and low-temperature coefficient of intrinsic coercivity [2]. It was known that the $SmCo_7$ phase is a metastable phase and a third element (M = Ga, Hf, Ti, Zr, etc.) is needed to stabilize it [3–6]. Further investigations show that melt spinning and mechanical alloying are two effective methods to obtain nanocrystalline $SmCo_7$ magnets with very high coercivity [7] and mechanical alloying is more effective to produce nanocrystalline SmCo magnets [8]. Magnetic properties and microstructure of $SmCo_7$ compound have been studied systematically [3,9–11]. Saito et al. [11] reported that $Sm_2(Co, Mn)_{17}$ magnet with the $TbCu_7$ structure exhibits an anisotropy field of 105–140 kOe, which is 1.2–1.4 times larger than that of $Sm_2(Co, Mn)_{17}$ with the Th_2Zn_{17} structure [11]. $SmCo_7$ phase also plays an important role in developing the cellular structure in 2:17-type $Sm(Co, Fe, Cu, Zr)_z$ magnet, leading to high coercivity. It is well known that magnetic properties of permanent magnetic materials and their temperature dependence are related to the magnetization reversal mechanism. In order to further improve the high temperature properties, more investigation on the coercivity mechanism of nanocrystalline $SmCo_7$ compound is necessary.

In this paper, the Zr-doped $SmCo_7$ based nanocrystalline magnets are synthesized by mechanical alloying and subsequent annealing. Structure, magnetic properties and magnetization reversal process of them are investigated systematically.

2. Experimental procedures

The $SmCo_{6.8}Zr_{0.2}$ alloy was prepared by arc melting. An excess Sm of 10 wt% was added to compensate for the weight loss due to Sm evaporation. The alloy was melted for four times to ensure homogeneity. The as-cast alloy was crushed into coarse powder with typical sizes less than 180 μm. The coarse powder was milled for 10 h under argon atmosphere using a high-energy mill of Spex 8000 with a ratio of powder to ball of 1:2. The as-milled powder was subsequently annealed at 600–900 °C for 3–30 min.

The phase compositions were determined by X-ray diffraction (XRD) of Bruker AXS with Co Kα radiation. The magnetic properties and the magnetization reversal process of resin-boned magnets produced from the powders were measured using a Physical Property Measurement System (PPMS-9) of Quantum Design model 9 with a maximum field of 9 T at room temperature. No correction was made for the demagnetization field effect.

3. Results and discussion

3.1. Phase analysis

XRD patterns of the $SmCo_{6.8}Zr_{0.2}$ powders annealed for 10 min at different temperatures are shown in Fig. 1. It can be seen that the as-milled powder are nearly amorphous and a single phase

* Corresponding author.
E-mail address: zliu@nimte.ac.cn (Z. Liu).

0925-8388/$ – see front matter © 2011 Elsevier B.V. All rights reserved.
doi:10.1016/j.jallcom.2010.12.192

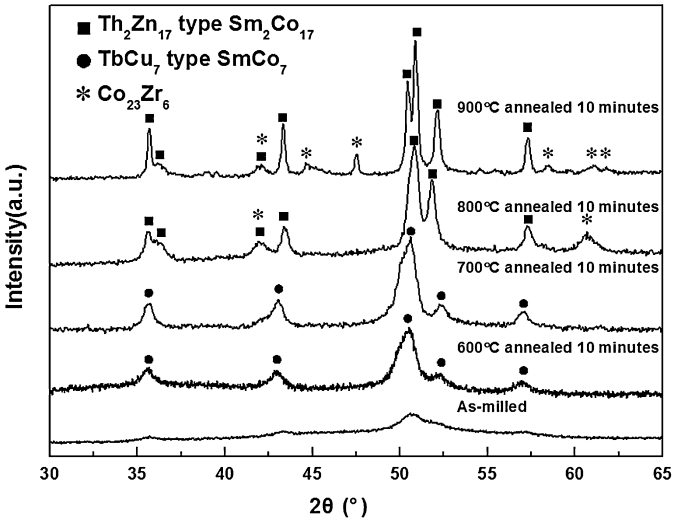

Fig. 1. XRD patterns of as-milled $SmCo_{6.8}Zr_{0.2}$ powders annealed at 600 °C, 700 °C, 800 °C and 900 °C for 10 min.

with $TbCu_7$ structure is obtained in the samples annealed at 600 °C and 700 °C. Higher annealing temperatures lead to the formation of Sm_2Co_{17} and $Co_{23}Zr_6$ phases, as well as larger grain size. According to Scherrer method, the mean grain sizes of $SmCo_{6.8}Zr_{0.2}$ alloys in the samples annealed at 600 °C, 700 °C, 800 °C and 900 °C for 10 min are about 18 nm, 25 nm, 45 nm and 65 nm, respectively. It is obvious that the annealing temperature has a significant effect on the phase composition of the magnets.

Fig. 2(a)–(c) shows the XRD patterns of samples annealed at 600 °C, 700 °C and 800 °C for different time, respectively. According to Fig. 2(a), annealing time has no effect on the phase structure and a single $SmCo_7$ phase is observed for samples annealed at 600 °C for different annealing time. When the annealing temperature is increased to 700 °C, a small amount of Th_2Zn_{17}-type Sm_2Co_{17} phase is detected with the annealing time increasing up to 20 min, as shown in Fig. 2(b). The thermomagnetic curves (M–T) of two samples annealed at 700 °C for 10 and 20 min are shown in Fig. 2(d). It can be seen that three Curie temperatures of T_{c1} (700–800 °C), T_{c2} (800–900 °C) and T_{c3} (>1000 °C) are observed, which should be the Curie temperatures of $SmCo_7$, Sm_2Co_{17} and Co phases, respectively. It can be clearly seen that the Sm_2Co_{17} phase is observed in the sample annealed for 20 min, while it is not detected in the sample annealed for 10 min. It is consistent with the analysis result

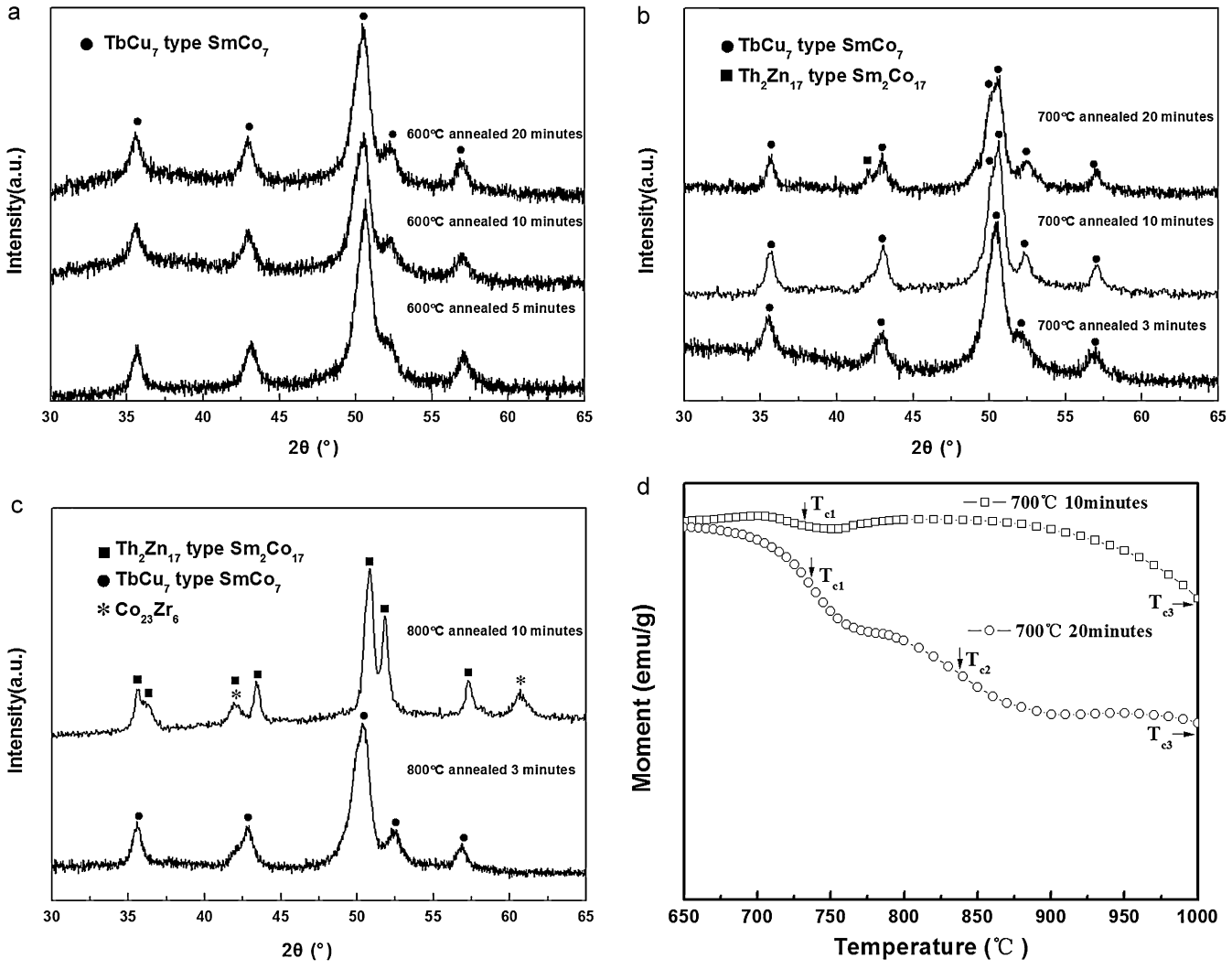

Fig. 2. XRD patterns of as-milled $SmCo_{6.8}Zr_{0.2}$ powders (a) annealed at 600 °C for different annealed time. (b) Annealed at 700 °C for different annealed time. (c) Annealed at 800 °C for 3 and 10 min. (d) The thermomagnetic curves (M–T) of sample annealed at 700 °C for 10 and 20 min.

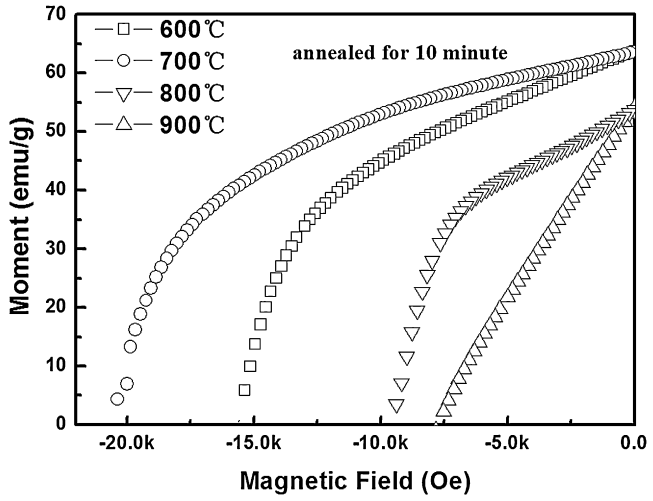

Fig. 3. Demagnetization curves for mechanically milled sample annealed 10 min with different temperature.

of Fig. 2(b). From Fig. 2(c), with the annealing temperature further increasing, a single phase of $TbCu_7$-type is obtained for as-milled $SmCo_{6.8}Zr_{0.2}$ sample annealed at 800 °C for 3 min and the $SmCo_7$ phase transforms to a mixture of Th_2Zn_{17} and $Co_{23}Zr_6$ phases with annealing time increasing to 10 min.

3.2. Magnetic properties

Fig. 3 shows the demagnetization curves of the samples annealed at different temperatures for 10 min. It can be seen that the coercivity first increases and then decreases with annealing temperature increasing. The highest coercivity of about 2.06 T is obtained in the sample annealed at 700 °C for 10 min. A small kink is observed in the demagnetization curves of samples annealed at 800 °C and 900 °C for 10 min, which may be due to the coarse grain size of Sm_2Co_{17} phase.

Fig. 4(a) and (b) shows the dependence of coercivity and energy product of the annealed sample on annealing time, respectively. From Fig. 4(a), it can be seen that coercivity increases monotonically with annealing temperature increasing from 600 °C to 800 °C within 5 min. When the annealing time exceed 5 min, coercivity starts to decrease for samples annealed at higher temperature (>700 °C), which is mainly due to the appearance of Tb_2Zn_{17}-type Sm_2Co_{17} phase (see Fig. 2(b) and (c)), which have much lower magnetic anisotropy field than $TbCu_7$ type $SmCo_7$ phase, as indicated in Fig. 2(d). The energy product is first increase and then decrease in the samples annealed at 600 °C, 700 °C and 800 °C. When the samples are annealed at and 900 °C, the energy product of samples are monotonically decreased with the annealed time. The highest energy product of about 9.5MGOe is obtained in sample annealed at 700 °C for 10 min.

3.3. Magnetization reversal behavior

In order to understand the magnetization reversal of nanocrystalline $SmCo_{6.8}Zr_{0.2}$ magnets, the magnetization behaviors of $SmCo_{6.8}Zr_{0.2}$ sample annealed at 700 °C for 3 min (SZ-3) and annealed at 700 °C for 10 min (SZ-10) are further investigated.

As for the nucleation controlled reversal magnetization [12], domain walls move easily inside grains. Hence a larger initial permeability than that of domain pinning mechanism is expected. The coercivity increases already in a relatively small magnetizing field. Technical saturation is reached in the magnetizing field that is substantially lower than the induced coercivity. Furthermore,

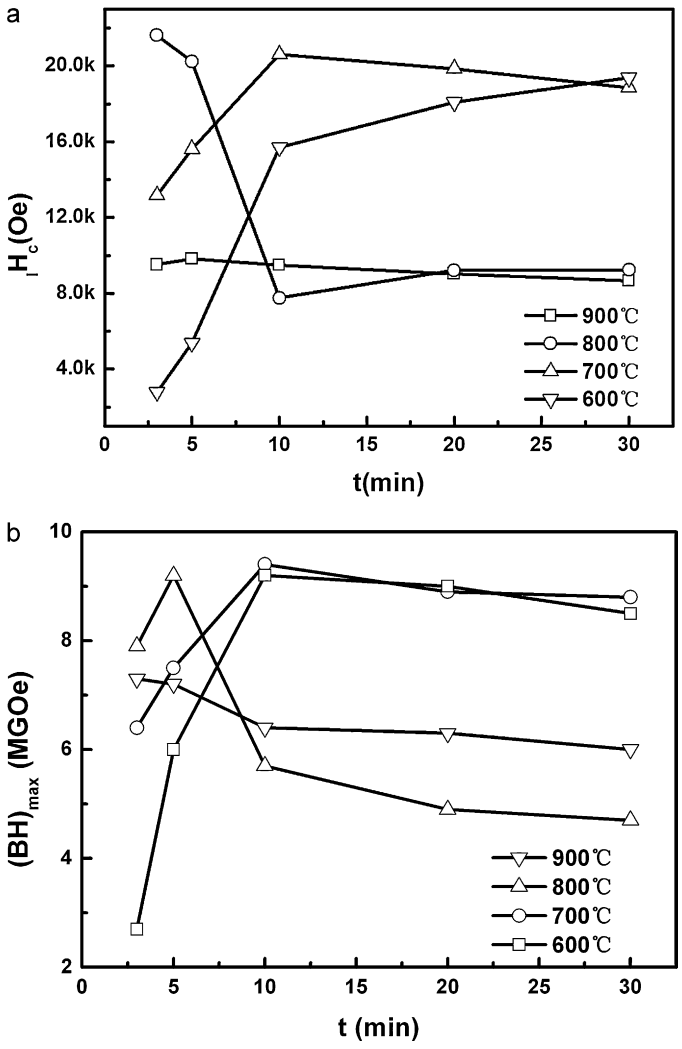

Fig. 4. Coercivity (a) and energy product (b) of $SmCo_{6.8}Zr_{0.2}$ powders as a function of different annealed time from 3 to 30 min at different annealed temperature.

the increase of the remanence is faster than that of the coercivity with increasing magnetizing field. In contrast, the situation is quite different for homogeneous pinning model. Because domain walls are pinned, the initial magnetization cure is almost horizontal at first and then builds up to intrinsic coercivity. Remanence and coercivity remain unchangeable for small magnetizing field and then they increase to saturation drastically when the magnetizing field reaches the intrinsic coercivity [13]. The increase of the coercivity with increasing magnetizing field is faster than that of remanence [13]. The initial magnetization curves for ideal nucleation and homogeneous pinning model are also shown in Fig. 5. As shown in Fig. 5, the rise of initial magnetization curve is low. When the magnetizing field H reaches the value of $_iH_c$, $M(H)$ is about $0.5M_s$. Even though H reaches the value of $2\ _iH_c$, $M(H)$ is still smaller than $0.9M_s$, which indicates that the magnetization reversal behavior of SZ-3 sample is controlled by inhomogeneous pinning model. It can also be seen in the analysis of minor hysteresis loops of $SmCo_{6.8}Zr_{0.2}$ sample annealed at 700 °C for 3 min (SZ-3) shown in Fig. 6(a). The field dependence of the reduced remanence $(J_r(H)/J_r)$ and coercivity $(H_c/{}_iH_c)$ obtained from the minor hysteresis loops of SZ-3 powder are shown in Fig. 6(b), where the $J_r(H)$ is acquired after the application and subsequent removal of H, H_c is acquired after the application and turn to –H, J_r is the saturated remanence, and $_iH_c$ is the intrinsic coercivity. As shown in Fig. 6(b), the values of $J_r(H)/J_r$ and $H_c/{}_iH_c$ is low at $H/{}_iH_c < 0.9$, However, it grows rapidly

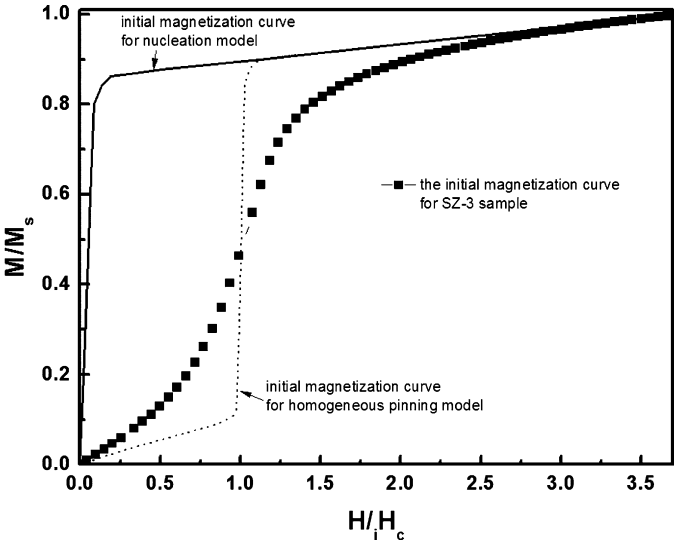

Fig. 5. The initial magnetization curve for SZ-3 sample and the initial magnetization curve for ideal nucleation and homogeneous pinning model.

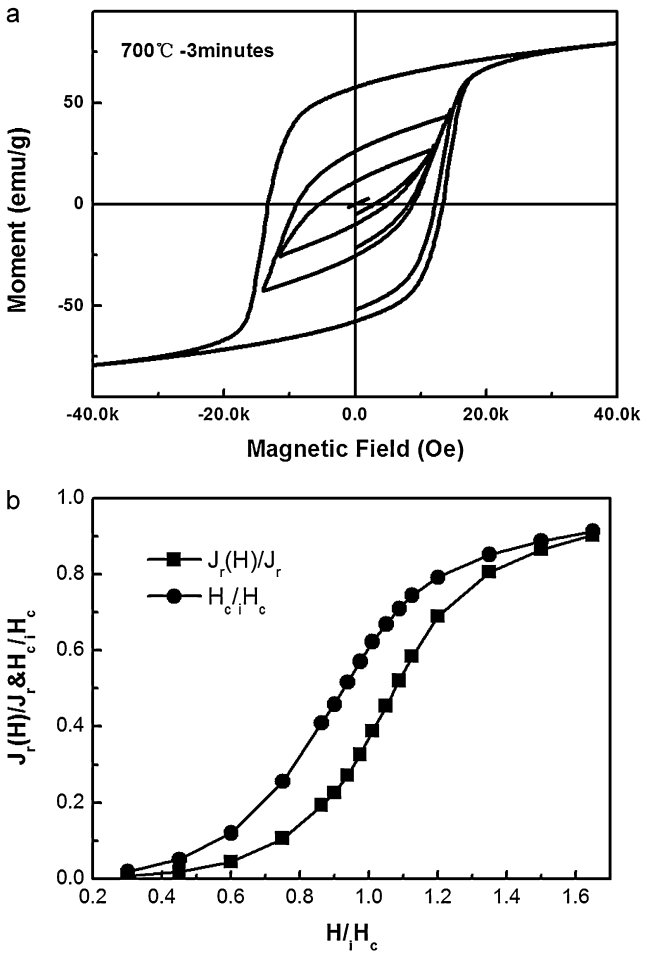

Fig. 6. (a) Minor hysteresis loops of SZ-3 powders and (b) J_r (H)/J_r and $H_c/_iH_c$ as function of the applied field $H/_iH_c$ of SZ-3 powders.

after a critical field ($H/_iH_c > 0.9$) is reached, which is the typical features of domain wall pinning [13,14]. Furthermore, from the initial magnetization curve increases continuously within a wide range of magnetizing field, the developments of remanence and coercivity are not expected for the homogeneous pinning as well. It suggests

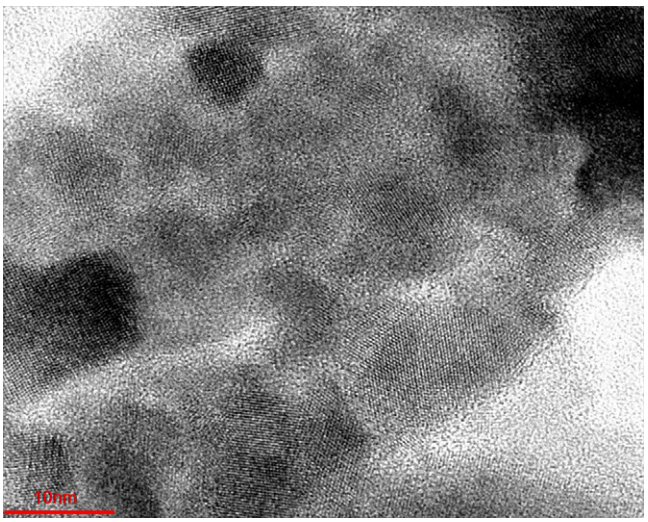

Fig. 7. TEM picture for SZ-3 sample.

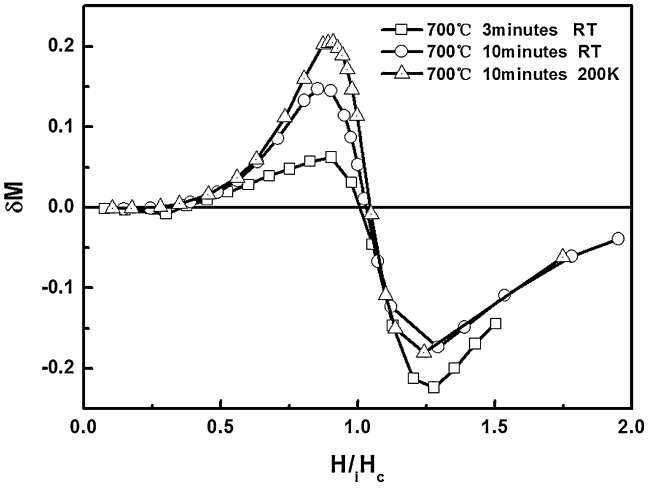

Fig. 8. Variation of $\delta m = \{J_d(H) + 2J_r(H) - J_r\}/J_r$ with the applied magnetic field for SZ-3, SZ-10 measured at room temperature (RT) and SZ-10 measured at 200 K.

that there is a wide distribution of the pinning strength in the SZ-3 sample. In other words, the coercivity mechanism is determined by the inhomogeneous domain wall pinning. Fig. 7 shows the TEM picture for SZ-3 sample. It can be obviously seen that the edge of crystal show atomic disorder with different width. These defects could be the pinning center of magnetic domain.

As shown in Fig. 6(a), the large remanence ratio J_r/J_s of 0.71 suggest that there is a strong inter-grain exchange coupling in SZ-3 sample [12]. The deviation of demagnetization remanence $J_d(H)$ from J_r–$2J_r(H)$ can also be used for interpretation of inter-grain interaction. Where the demagnetization remanence $J_d(H)$ is measured after demagnetization at $-H$ on the demagnetization curve. The deviation δm is defined as: $\delta m = \{J_d(H) + 2J_r(H) - J_r\}/J_r$. The δm–H curves of SZ-3, SZ-10 sample measured at room temperature (RT) and that of SZ-10 sample measured at 200 K are shown in Fig. 8. Nonzero δm is believed to be due to the interaction in a magnet and positive values of δm are due to inter-grain exchange coupling, while negative values of δm are reasonably due to the dipolar interaction [15,16]. The positive values of δm indicate the presence of the inter-grain exchange coupling in the nanocrystalline $SmCo_7$ magnets, as shown in Fig. 8. The larger peak value of the positive δm in SZ-10 sample at RT reveals a stronger inter-grain exchange coupling. The presence of amorphous in SZ-3 sample, confirmed by

XRD, weaken the inter-grain exchange coupling and thus results in poor magnetic properties. In addition, the inter-grain exchange coupling is getting stronger with measured temperature decreasing from RT to 200 K, indicating that thermal disturb can weaken inter-grain exchange coupling. The large negative values of δm are indicative of strong dipolar interactions in our researched samples, similar to that observed in the $SmCo_5/Sm_2Co_{17}$ nanocomposite system as reported in Ref. [17]. This may be due to the stray fields [18,19] originating from defects and non-ideal grain boundaries introduced by milling which prevents the exchange interaction.

4. Summary and conclusion

Nanocrystalline $SmCo_{6.8}Zr_{0.2}$ compound was fabricated by mechanical alloying and subsequently annealing. The highest coercivity above 20KOe was achieved in the nanocrystalline $SmCo_{6.8}Zr_{0.2}$ after milling for 10 h and being annealed at 700 °C for 10 min. The coercivity mechanism is mainly controlled by the domain wall pinning. Strong inter-grain exchange coupling is observed in SZ-3 and SZ-10 samples, which was verified by the J_r/J_s (>0.5) value and positive δm in the δm–H curve. Large negative δm indicates strong dipolar interactions which could be due to the stray fields originating from defects and non-ideal grain boundaries introduced by milling.

Acknowledgments

The work was supported by the Nature Scientific Foundation of Zhejiang Province, China with Grant No. Y407174 and the science and technology project of Zhejiang Province, China with Grant No. 2007C21097. The authors thank Mr. Li Ming for the help in PPMS measurement and Mr. Huang Qin for the help in XRD analysis.

References

[1] J.F. Liu, T. Chui, D. Dimitrov, G.C. Hadjipanayis, Appl. Phys. Lett. 73 (1998) 3007.
[2] D.T. Zhang, M. Yue, L.J. Pan, Y.C. Li, G. Xu, W.Q. Liu, J.X. Zhang, X.B. Liu, Z. Altounian, J. Appl. Phys. 103 (2008) 07E124.
[3] M.Q. Huang, W.E. Wallace, M. McHenry, Q. Chen, B.M. Ma, J. Appl. Phys. 83 (1998) 6718.
[4] J. Zhou, R. Skomski, C. Chen, G.C. Hadlipanayis, D.J. Sellmyer, Appl. Phys. Lett. 77 (2000) 1514.
[5] I.A. Al-Omari, Y. Yeshurun, J. Zhou, D.J. Sellmyer, J. Appl. Phys. 87 (2000) 6710.
[6] Y.Q. Guo, W. Li, W.C. Feng, J. Luo, J.K. Liang, Q.J. He, X.J. Yu, Appl. Phys. Lett. 86 (2005) 192513.
[7] S.K. Chen, M.S. Chu, J.L. Tsai, T.S. Chin, IEEE Trans. Magn. 32 (1996) 4419.
[8] C.B. Jiang, M. Venkatesan, K. Gallagher, J.M.D. Coey, J. Magn. Magn. Mater. 236 (2001) 49.
[9] M. Venkatesan, F.M.F. Rhen, R. Gunning, J.M.D. Coey, IEEE Trans. Magn. 38 (2002) 2919.
[10] Z. Yao, P.P. Li, C.B. Jiang, J. Magn. Magn. Mater. 321 (2009) 203–206.
[11] H. Saito, M. Takahashi, T. Wakiyama, G. Kodoand, H. Nakagawa, J. Magn. Magn. Mater. 82 (1989) 322.
[12] F.E. Pinkerton, D.J. Van Wingerden, J. Appl. Phys. 60 (1996) 3685.
[13] K.H.J. Buschow, Rep. Prog. Phys. 54 (1991) 1123.
[14] J.F. Liu, H.L. Luo, J. Wan, J. Pediatr. (St. Louis) 25 (1992) 1238.
[15] P.E. Kelly, K.O. Grady, P.I. Mayo, R.W. Chantrell, IEEE Trans. Magn. 25 (1989) 3881.
[16] H.W. Zhang, C.B. Rong, X.B. Du, J. Zhang, S.Y. Zhang, B.G. Shen, Appl. Phys. Lett. 82 (2003) 4098–4100.
[17] A. Yan, A. Bollero, O. Gutfleisch, K.H. Muller, J. Appl. Phys. 91 (2002) 2192.
[18] R. Fisher, H. Kronmu¨ller, J. Appl. Phys. 83 (1998) 3271.
[19] V. Neu, A. Hubert, L. Schultz, J. Magn. Magn. Mater. 189 (1998) 391–396.